

CONTROLLING THE VERTICAL EMITTANCE COUPLING IN CAMD

M Fedurin, P Jines, D Launey, T Miller, V Suller, Y Wang; CAMD, Baton Rouge LA 70806, USA

Abstract

The vertical beam size in the CAMD Light Source, as measured with an X-ray pinhole camera, indicates an emittance coupling ratio of about 1.5%. The coupling parameter has been measured by the betatron tune split when the coupling resonance is fully engaged. It is found that the coupling is increased by the 7 Tesla wiggler, which is known to contain non-linear fields. Attempts to reduce the vertical beam size with a skew quadrupole have not succeeded. It is possible that spurious vertical dispersion and image blurring make large contributions to vertical size measurements.

CONTROLLING THE VERTICAL EMITTANCE COUPLING IN CAMD

M Fedurin, P Jines, D Launey, T Miller, V Suller, Y Wang; CAMD, Baton Rouge LA 70806, USA

Abstract

The vertical beam size in the CAMD Light Source, as measured with an X-ray pinhole camera, indicates an emittance coupling ratio of about 1.5%. The coupling parameter has been measured by the betatron tune split when the coupling resonance is fully engaged. It is found that the coupling is increased by the 7 Tesla wiggler, which is known to contain non-linear fields. Attempts to reduce the vertical beam size with a skew quadrupole have not succeeded. It is possible that spurious vertical dispersion and image blurring make large contributions to vertical size measurements.

BEAM SIZE MEASUREMENT

Although the CAMD Light Source [1] was initially used mostly for lithography, its growing research program now requires good source flux density and brightness. Tuning the lattice has given higher brightness by reducing the emittance and the use of an optic with a mini-beta at the 7 Tesla wiggler gives high flux density. Scope for further increases is probably limited to reducing the vertical beam size by minimizing the emittance coupling ratio.

The profile of the electron beam in the storage ring is observed by focusing the visible synchrotron radiation directly onto a CCD array. The light is reflected downwards by a cooled silicon mirror and exits the vacuum chamber through a glass window. A second mirror returns the beam to the horizontal and a 500 mm focal length glass lens produces the required image of the source point. Neutral density filters control the beam intensity to prevent saturation of the CCD array, which is mounted with its line scan direction aligned vertically. This results in the best possible resolution of the vertical dimension of the image.

This visible image of the electron beam source is excellent for giving qualitative information of the source size from injection energy, through the energy ramp, and during User beam. It can only give limited quantitative information about the source dimensions because of uncertainty about the exact figure of the mirror under the heat load of the X-ray component of the incident beam, and by diffraction limitations in the vertical plane.

To provide more precise measurement of the beam dimensions an X-ray pinhole camera is used. The radiation source point is near the centre of a dipole and about 20 mm of horizontal beam emerges through a 1 mm thick beryllium window. The pinhole is located 2.29 m from the source and the distance from it to the imaging screen, made of Calcium Tungstate, is 1.235 m. The interchangeable pinhole is in 100 μm thick platinum and normally a diameter of 50 μm is used. The vertical position of the pinhole is remotely adjustable so that it can be exactly centered in the vertical radiation fan. The

image is viewed highly magnified by a CCD TV camera and to prevent saturation of the signal at 200mA electron beam current, an aluminum attenuator 0.6 mm thick is placed in the X-ray path.

In making a measurement of the beam size the pinhole image is captured by a commercial frame-grabber. This is then analyzed by software which allows cursors to be positioned at selected points on the profile. Best accuracy is given by measuring the full width of the profile at 25% of the peak height. A calibration grid on the image screen enables the profile width measured in pixels to be related to real mms. An example of the analysis of a pinhole camera image is shown in Fig. 1.

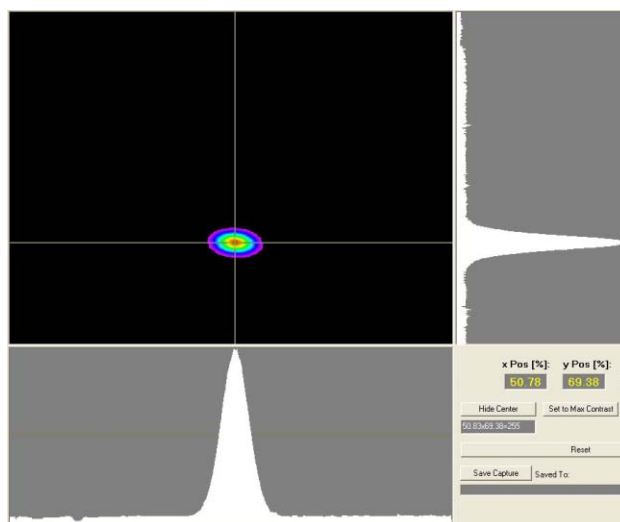


Figure 1: Analysis of an X-ray pinhole camera image.

From the measured image size the dimensions of the source are calculated. The demagnification of the pinhole camera is determined by physical measurement of the source to pinhole and pinhole to screen distances. Corrections are applied for pinhole diffraction and blurring. The pinhole diameter was measured with a calibrated microscope. It is estimated that a vertical source sigma of 200 μm can be measured with a precision better than 20 μm . The principal uncertainty is the image blurring contributed by the Calcium Tungstate image screen. A typical beam size (horizontal x vertical sigmas) measured at 150 mA with the wiggler at 7 Tesla is 0.49 mm x 0.24 mm.

COUPLING

The theory of linear betatron coupling [2] shows that the ratio g of the vertical to horizontal emittances is given

$$g = \frac{C^2}{C^2 + 2\Delta^2}$$

where the coupling parameter C is measured by the closest approach of the betatron tunes to the coupling resonance and Δ is the magnitude of the tune separation from the coupling resonance at the operating point.

The coupling parameter in CAMD has been measured for the 3 principal operating optics, namely; symmetric zero dispersion; and minibeta with the wiggler either off or at 7 Tesla. These are given in Table 1. An example of the data for the case of the wiggler at 7 Tesla is shown in Fig. 2.

Table 1: Measured values of the Coupling parameter

Lattice configuration	Coupling parameter
Symmetric zero dispersion	0.005
Minibeta wiggler off	0.006
Minibeta wiggler 7 Tesla	0.010

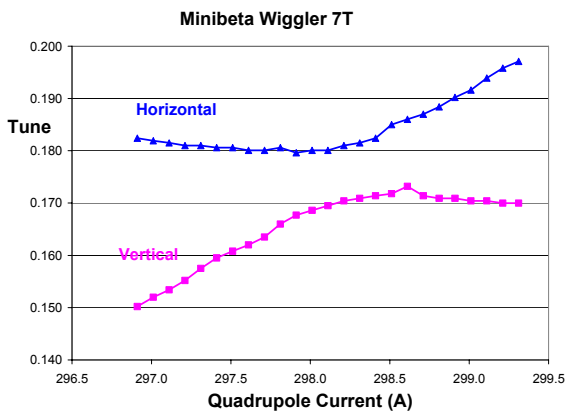


Figure 2: A measurement of the coupling parameter with the wiggler at 7Tesla.

From the relationship given earlier for the emittance coupling ratio it is clear that the ratio reduces the further the operating tune point lies from the coupling resonance. In CAMD this is the resonance:-

$$Q_H - Q_V = 2$$

The operating betatron tunes have been selected to be horizontal 3.238 and vertical 1.145, in order to be far from this resonance line. The expected emittance ratios are calculated to range from 0.15% in the symmetric zero dispersion case to 0.6% with minibeta and 7 Tesla wiggler.

X-ray Pinhole camera measurements of the horizontal beam size are in reasonable agreement with the values calculated by the lattice model. The measured vertical sizes, however, are not consistent with those expected from the coupling ratios derived from the measured values of the coupling parameter. The vertical sizes are shown in Table 2.

The measured vertical sigmas are consistently larger than expected given the separation of the working tune point from the coupling resonance. If the tune point is moved close to the coupling resonance the vertical beam size does increase as given by the formula for the coupling ratio.

Table 2: Measured and calculated vertical beam sizes

Lattice configuration	Calculated sigma v (μm)	Measured sigma v (μm)
Symmetric zero dispersion	70	220
Minibeta wiggler off	80	250
Minibeta wiggler 7 Tesla	140	240

MULTIPOLE MAGNET

A small 12 pole magnet with independent power supplies for each of its coils has been installed in the storage ring [3]. By suitably energizing these coils a range of useful multipole fields can be produced, including skew quadrupole. It is intended that 4 of these magnets will eventually be installed to assist with beam optimization and control, and especially to compensate for the non-linear fields produced by the wiggler. A photo of the multipole magnet is shown in Fig. 3.

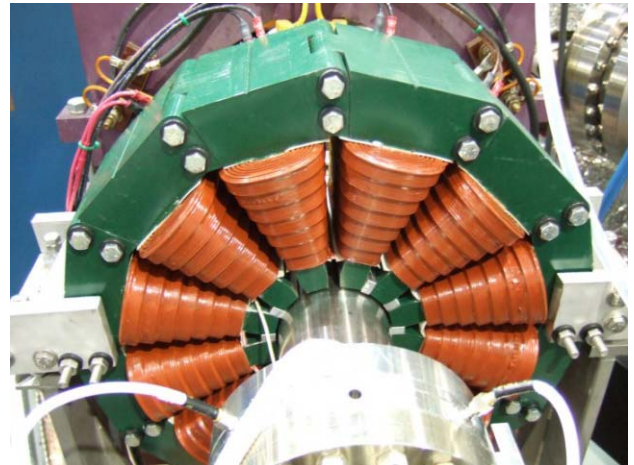


Figure 3: A view of the prototype multipole magnet after installation in the storage ring.

The multipole magnet has been used as a skew quadrupole and tested for its effect on the coupling parameter and the vertical beam size. Its effect in reducing the coupling parameter can be seen in Fig. 4 where for a specific value of the skew quadrupole field the coupling parameter in minibeta with the wiggler on at 7 Tesla the coupling has been essentially reduced to zero. Similar cancellation, with lower current in the multipole, is found for the other lattice optics.

However, it has been found that despite the coupling parameter being cancelled by the skew quadrupole the vertical beam size is not reduced. The normal elliptical beam image is seen to become rotated with respect to the horizontal plane, see Fig. 5, as the skew quadrupole is increased, as would be expected from a single lumped multipole in the lattice. At no point did the skew quadrupole reduce the vertical beam size.

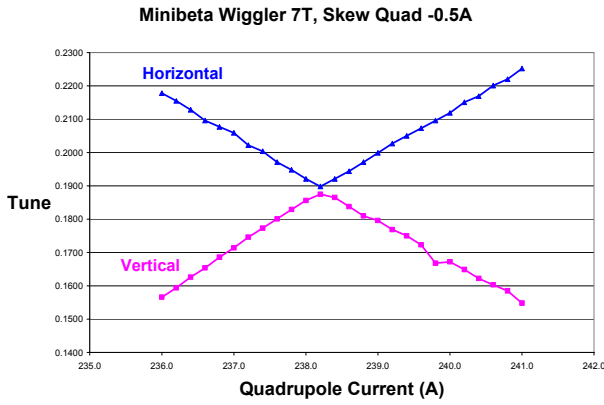


Figure 4: Cancellation of the coupling parameter with the wiggler at 7Tesla by the skew quadrupole.

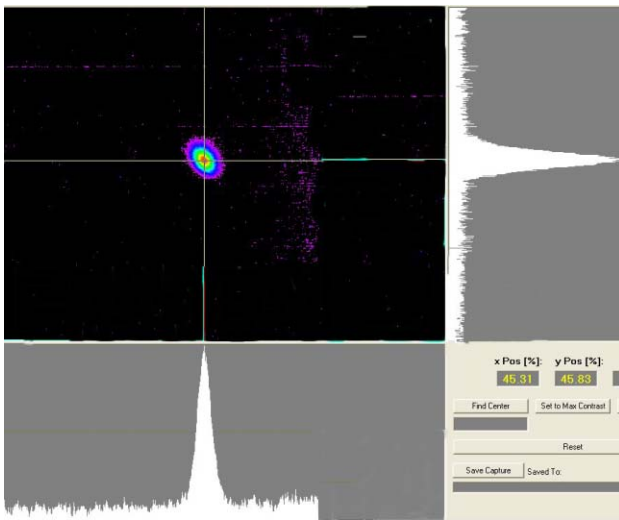


Figure 5: Rotated beam image due to the skew quadrupole.

CONCLUSIONS

The measured values of the coupling parameter and its behavior as the wiggler is powered suggest that it is correctly representing the real coupling in the storage ring. Furthermore, its cancellation using a single skew quadrupole can be precisely measured and is consistent with the coupling in the different lattice configurations.

The fact that the vertical beam size as measured is larger than expected from the coupling and that it does not decrease when the coupling is cancelled by a skew quadrupole is suggestive of some different mechanism contributing to the vertical beam size. The most likely candidate is spurious vertical dispersion, but to account entirely for the measured vertical size the dispersion would need to be significantly larger than measured (0.2 m compared with 0.05 m). Furthermore, the measured, larger than expected, beam size cannot be totally attributed to blurring by the X-ray imaging screen, which may contribute at most 50 μm to the size.

These effects will receive continued attention until the vertical beam size can be quantified with full confidence.

REFERENCES

- [1] BC Craft et al., NIM B-40/41, p373, (1989); V P Suller et al., Proceedings of EPAC'04, Lucerne, 2004, pp 2424-2426.
- [2] G Guinard; CERN Accelerator School Advanced Course 1993; CERN 95-06, vol 1. pp 61-63.
- [3] M Fedurin et al., Proceedings of PAC05, Knoxville, 2005, pp 3161-3163.